Microstructure and Magnetic Properties of Carbon-Coated Nanoparticles

1 AUTHOR:

Xiangcheng Sun
University of Waterloo
86 PUBLICATIONS   **844** CITATIONS

SEE PROFILE

Microstructure and Magnetic Properties of Fe(C) and Fe(O) Nanoparticles

Xiang-Cheng Sun*,[†] and N. Nava[‡]

Center for Materials for Information Technology (MINT), The University of Alabama, P.O. Box 870209, Tuscaloosa Alabama, 35487-0209, and Instituto Mexicano del Petroleo, Central Lazaro Cardenas 152, 07730, D. F. Mexico

ABSTRACT

Both Fe(C) and Fe(O) nanoparticles have been successfully synthesized using a modified graphite arc-discharge method. X-ray diffraction (XRD), high-resolution transmission electron microscopy (HREM), and electron diffraction (SAED) analyses indicated that both of these Fe nanoparticles have an average grain size of 15–20 nm and α-Fe, γ-Fe, and Fe_3C phases are clearly identified in those Fe(C) particles, while an α-Fe and oxide layer (Fe_3O_4) are revealed in these Fe(O) particles. Mössbauer spectra and hyperfine magnetic fields at room temperature (RT) further confirm their distinct nanophases. At RT, the assemblies of Fe(O) nanoparticles exhibit ferromagnetic properties due to magnetocrystalline anisotropy effects. However, modified superparamagnetic relaxation is observed in the assemblies of Fe(C) nanoparticles.

Nanoscale magnetic materials show novel properties that are markedly different from those of the bulk due to their very small sizes and fundamental change in the coordination, symmetry, and confinement.[1] Research on nanoscale magnetic Fe, Co, and Ni particles/clusters has been fairly active in the past decades because of their fundamental properties and potential applications to high-density magnetic recording media, color imaging, ferrofluids, and magnetic refrigeration.[2−5] In fact, the intrinsic magnetic properties are strongly influenced by the particle size; nanoscale magnetic particles usually exhibit specific properties such as superparamagnetism and quantum tunneling of magnetization,[6,7] which are regarded as unique features of magnetic nanoparticles. However, the formation of an antiferromagnetic oxide surface shell around ferromagnetic metal nanoparticles causes a magnetic exchange interaction that influences significantly the magnetic behavior of these particles.[8] Moreover, some novel magnetic system of carbon encapsulated ferromagnetic materials, e.g., Fe, Co, and Ni, had successfully been obtained by a number of researchers.[9−11] Interest was paid to the properties of the encapsulated particles, in particular to those involving novel magnetic properties of ferromagnetic materials. Therefore, it offers us an opportunity to produce similar alternative encapsulated ferromagnetic materials with a protective carbon layer around them. In other words, these carbon encapsulated magnetic materials should be considered to become good candidates for studying magnetization processes, magnetic anisotropy,[12] superparamagnetism,[6,13,14] and quantum relaxation of the magnetization.[15]

In this study, we herein use the modified graphite arc-discharge method to generate two types of iron nanoparticles (Fe(C) and Fe(O) nanoparticles) in methane and a mixture of H_2 and Ar atmospheres, respectively. X-ray diffraction, high-resolution transmission electron microscopy (HREM), and nanoarea electron diffraction are used to investigate their remarkable microstructure properties. Furthermore, magnetic behavior has been studied using a Mössbauer magnetometer at room temperature. The relationships between the microstructures and novel magnetic behavior are also discussed.
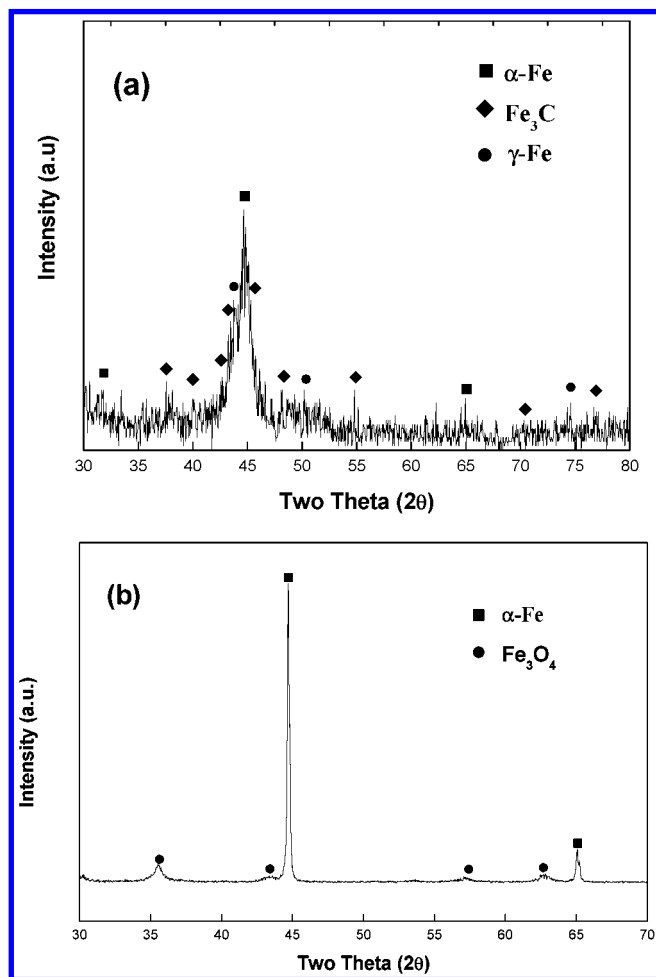
The experimental apparatus (modified graphite arc-discharge) was illustrated in elsewhere.[16−18] The pure material to be evaporated was laid on a water-cooled copper stage, which served as the anode. A copper arm that was also water-cooled supported the upper graphite rod, which served as the cathode. After the chamber was evacuated, the desired gas of methane and a mixture of H_2 and Ar were backfilled as a reactant gas to reach the desired pressure. The distance between the two electrodes can be adjusted from outside the chamber, so that the arc can be started and controlled during a continuous operation.

The grain size and morphologies of these Fe nanoparticles were studied by HREM and electron diffraction (SAED) performed on a JEOL-2010EX operated at 200 keV. X-ray

* Corresponding author. Tel: 205-348-2280, Fax: 205-348-2346, E-mail: xcsun@bama.ua.edu.
† The University of Alabama.
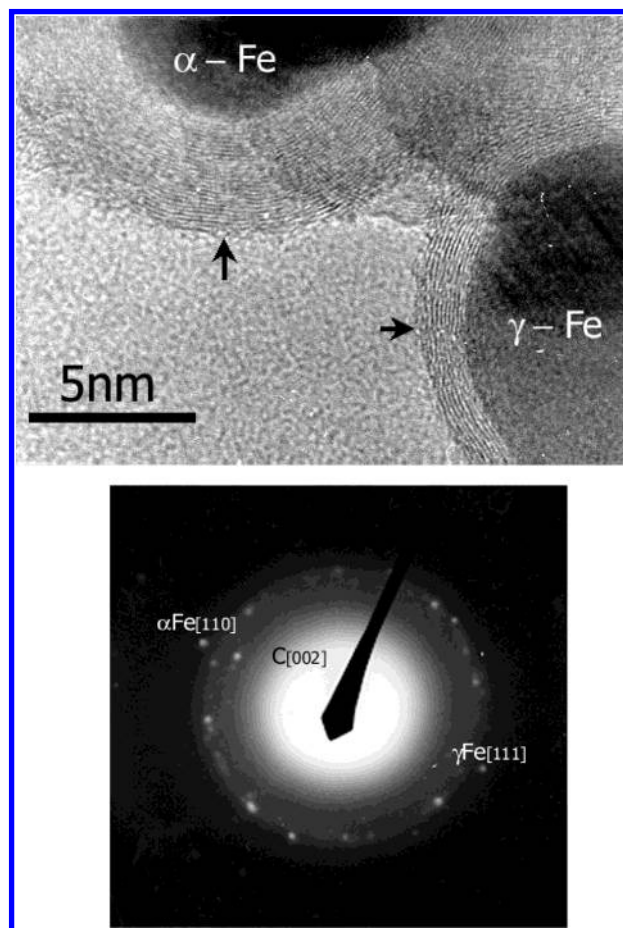‡ Instituto Mexicano del Petroleo.

Figure 1. Powder XRD patterns for Fe(C) nanoparticles (a) and Fe(O) nanoparticles (b).

Figure 2. Typical HREM image and SAED patterns for α-Fe(C) and γ-Fe(C) nanoparticles. Note that arrows indicate the carbon layers.

diffraction (XRD) was conducted using CuKα radiation in a Siemens X-ray diffactometer to identify the different nanophases and the crystal structure of nanoparticles. Mössbauer spectra were recorded at room temperature using an Austin Science Associates model S-600 spectrometer with a ^{57}Co/Rh source. The absorption spectra were computer fitted by using the *NORMOS* program that used the input parameters as a first approximation to fit the experimental curve.

Powder X-ray diffraction patterns of both Fe(C) and Fe(O) nanoparticles are shown in Figure 1 a and Figure 1b, respectively. It is very apparent to reveal that α-Fe (bcc), γ-Fe (fcc), and Fe$_3$C (orthorhombic) nanophases are detected from the assemblies of Fe(C) nanoparticles; these three phases are usually found in similarly prepared Fe−C nanocomposites.[9,19] However, dominant α-Fe nanophases and a small amount of Fe$_3$O$_4$ phases are examined from the assemblies of Fe(O) nanoparticles.

As revealed by the HREM images of Figure 2 and Figure 3, these Fe(C) nanoparticles (α-Fe, γ-Fe, and carbide Fe$_3$C) are typically spherical in core−shell shape and completely encapsulated by the wrapping shell carbon layers, which thickness is uniform over the surface of each particle. The size of three core nanocrystals is generally 10 to 15 nm, and

note that 10 to 40 carbon layers (rather than a single carbon layer) tightly cover each core nanocrystals only.[19,20] Meanwhile, electron diffraction (SAED) patterns of Figure 2 and Figure 3 further confirm the presence of α-Fe, γ-Fe, and carbide Fe$_3$C nanophases that are covered with carbon layers. Especially, X-ray diffraction (XRD) and electron diffraction (SAED) patterns indicate that no intermediate phases are observed between the wrapping carbon layers and three core nanocrystals.[17] These striking structural properties are in good agreement with our previous work on other carbon coated transition metal particles.[16−18]
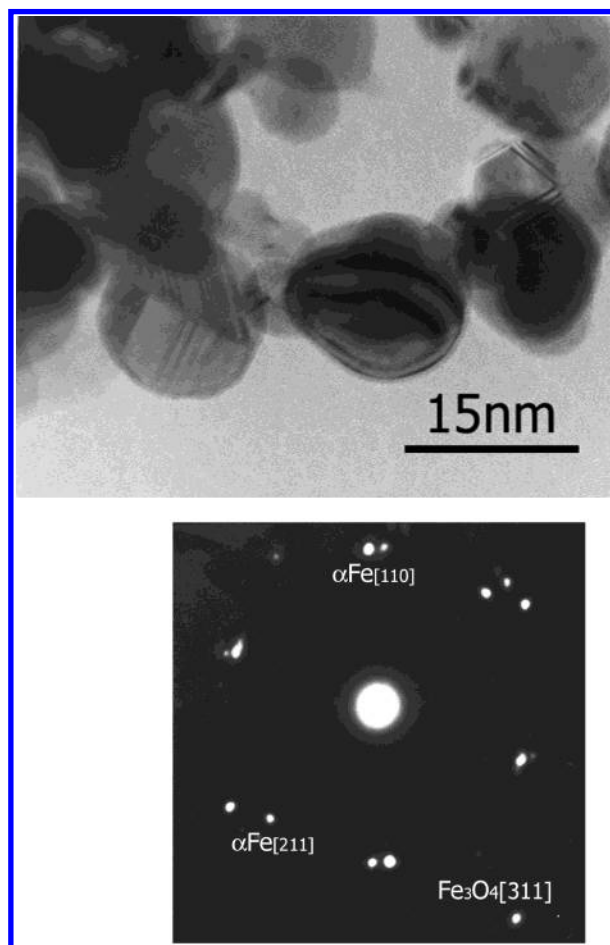
On the other hand, HREM images of Fe(O) nanoparticles in Figure 4 show that the particles are roughly spherical with many structure defects and slight distortion inside particle core. The particle size is about 15−20 nm. Electron diffractions patterns (SAED) in Figure 4 reveal the existence of α-Fe and Fe$_3$O$_4$ nanophases; moreover, additional diffuse SAED line patterns could be attributed to a few spinel-type Fe$_3$O$_4$ oxides that surrounding on the surface of these Fe(O) particles and reflect the presence of structure defects inside the particles.

Typical Mössbauer spectra and hyperfine fields of the assemblies of Fe(C) and Fe(O) nanoparticles at room temperature are showed in Figure 5. Spectra of Figure 5 (a, c) are fitted into the following components: the three sextets
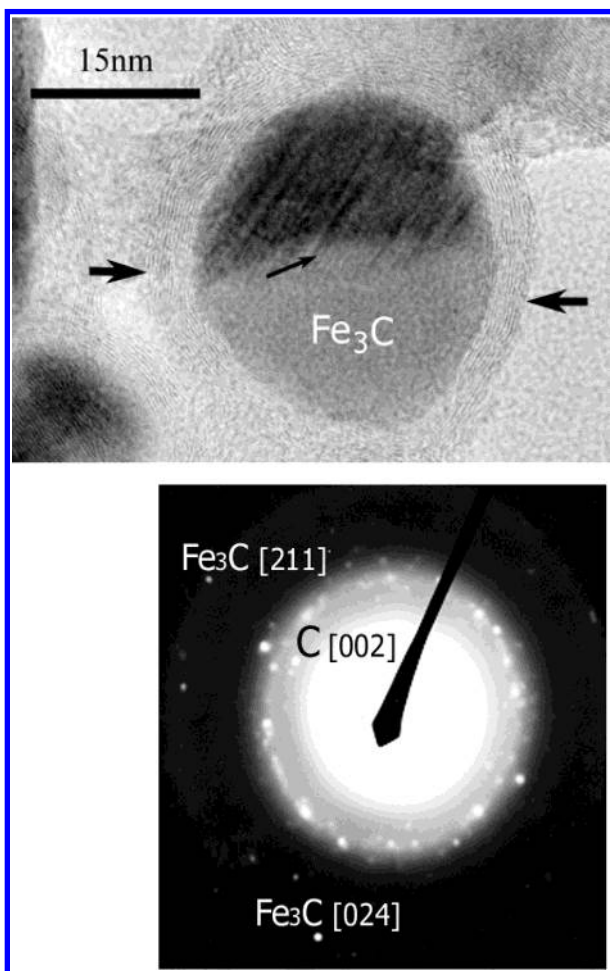
Figure 3. Typical HREM image and SAED patterns for Fe_3C phases in Fe(C) nanoparticles. Note that, arrows indicate the carbon layers and structure defects.

Figure 4. HREM image and SAED patterns for Fe(O) nanoparticles.

whose magnetic hyperfine field (H_{hyp}) values of 335 KOe, 271 KOe, and 200 KOe are assigned to α-Fe and two carbide Fe_3C nanophases, respectively.[9,21–23] Also, the singlet near zero velocity with an isomer shift (IS) = −0.126 mm/s is assigned to γ-Fe. On the other hand, Figure 5 (b, d) are decomposed into two phases: the two external sextets of low intensity with a magnetic field of 477 and 444 KOe are assigned to the Fe_3O_4 structure and the next internal intense sextet with a magnetic field of 320 KOe is assigned to α-Fe.[24,25] Generally speaking, Mössbauer spectra results at room temperature are in good agreement with that of the above XRD analysis and HREM observations, which confirm these distinct nanophases in both Fe nanoparticles. In addition, the evidence of modified superparamagnetic absorption peaks could be observed from Figure 5a at room temperature. However, such superparamagnetism can be blocked by interparticle dipole interactions due to the fact that the encapsulated particles are in contact with each other, which suggests that the assemblies of Fe(C) nanoparticles display modified superparamagnetic relaxation at room temperature.[22] Whereas, from Figure 5b, it can be seen that ferromagnetic properties at room temperature appear in the assemblies of Fe(O) nanoparticles, due to the increased magnetocrystalline anisotropy that originated from structure

defects and the coupling effects between the ferromagnetic α-Fe core and antiferromagnetic oxide (Fe_3O_4) shell layer in each particle.[12,17] As we know, from the HREM images of Figure 4, these Fe(O) nanoparticles are combined with the aligned necklace structure, thus, the magnetic moment of these particles couples with that of adjacent larger particles and becomes stable under thermal fluctuation. Therefore, it should not be surprising that the assemblies of Fe(O) nanoparticles display ferromagnetic properties at room temperature.

In summary, both iron (Fe) nanoparticles, Fe(C), and (Fe(O) nanoparticles have been presented. Microstructural features of two kinds of Fe nanoparticles have been characterized using X-ray diffraction, high-resolution transmission electron microscopy, and selected area electron diffraction analysis. It is demonstrated that the presence of carbon encapsulated α-Fe, γ-Fe, and Fe_3C phases are clearly identified in those Fe(C) particles; the evidence of pure α-Fe surrounded by an Fe oxide layer composed of Fe_3O_4 is examined in those Fe(O) particles.

Mössbauer spectra results at room temperature are in good agreement with that of above XRD and HREM analysis, which confirm these distinct nanophases in both Fe nanoparticles (Fe(C) and Fe(O)). It is very interesting to note that, at room temperature, the assemblies of Fe(O) nanoparticles
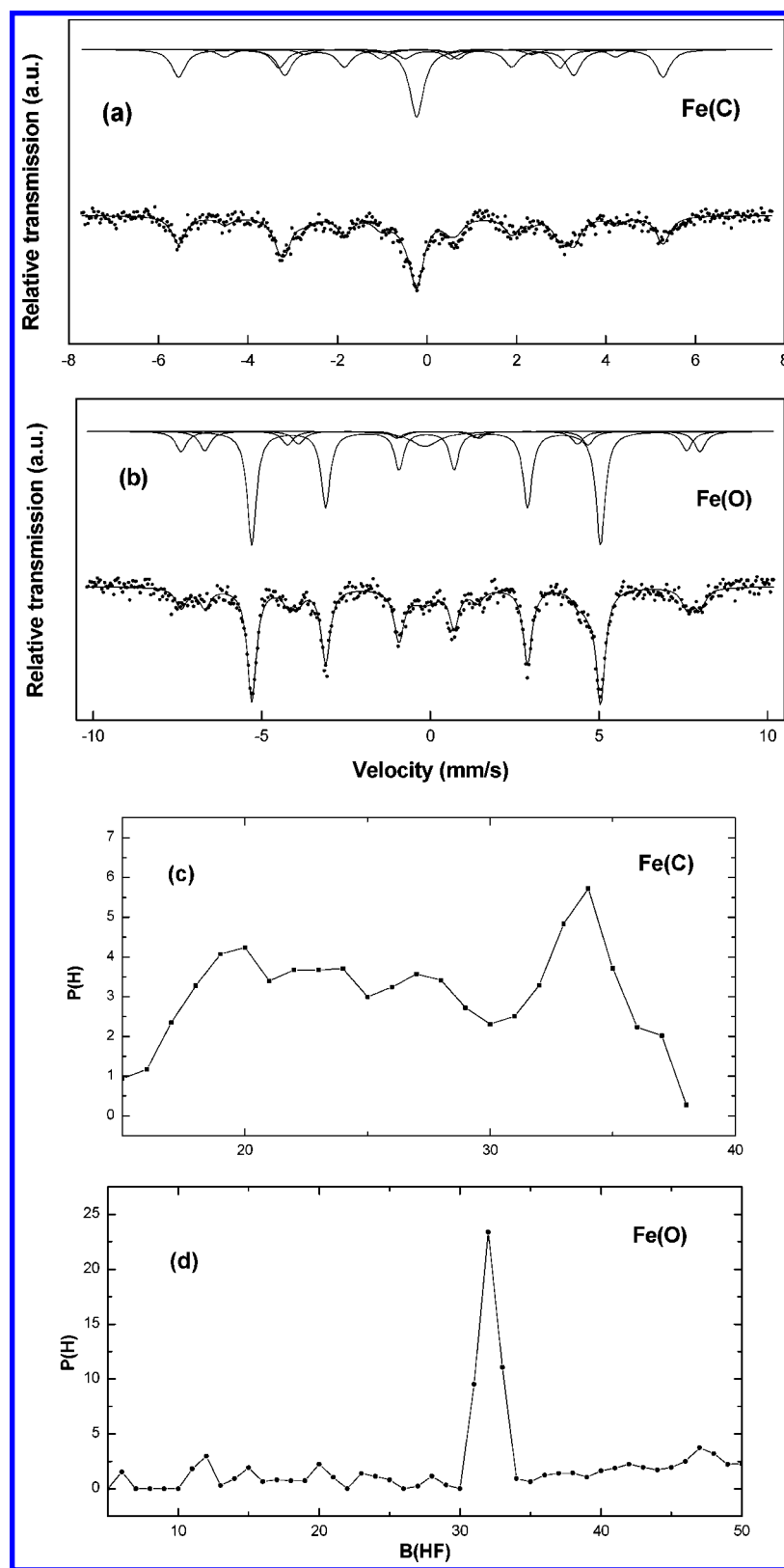
Figure 5. Mössbauer spectra (a, b) and hyperfine field distributions (c, d) for Fe(C) and Fe(O) nanoparticles, respectively.

display ferromagnetic properties due to the coupling interactions and magnetocrystalline effects; moreover, modified superparamagnetic relaxation is observed in the assemblies of Fe(C) nanoparticles. However, it is necessary to perform further studies on magnetization measurements, and confirm these specific magnetic properties.

References

(1) Leslie-Pelecky, D. L.; Rieke, R. D. *Chem. Mater.* **1996**, *8*, 1770.
(2) Dorman, J. L.; Fiorani, D. *Magnetic Properties of Fine Particles*; North-Holland: Amsterdam, 1992.
(3) Ziolo, R. F.; Giannelis, E. P.; Weinstein, B. A.; O'Horo, M. P.; Ganguly, B. N.; Mehrotra, V.; Russell, M. W.; Hufman, D. R. *Science* **1992**, *257*, 219.

(4) Awschalom, D. D.; DiVicenzo, D. P. *Phys. Today* **1995**, *4*, 43.

(5) McMichael, R. D.; Shull, R. D.; Swartzendruder, L. J.; Bennett, L. H.; Wastson, R. E. *J. Magn. Magn. Mater.* **1992**, *111*, 29.

(6) Chen, Q.; Zhang, Z. J. *Appl. Phys. Lett.* **1998**, *73*, 3156.

(7) Zhang, X. X.; Tejata, J.; Hernandez, J. M.; Ziolo, R. F. *Nanostruct. Mater.* **1997**, *9*, 301.

(8) Gangopadhyay, S.; Hadjipanayis, G. C. *J. Appl. Phys.* **1993**, *73*, 6964.

(9) Hihara, T.; Onodera, H.; Sumiyama, K.; Suzuki, K.; Kasuya, A.; Hishina, Y.; Satio, Y.; Yoshikawa, T.; Okuda, M. *Jpn. J. Appl. Phys.* **1994**, *33*, L24.

(10) McHenry, M. E.; Majetich, S. A.; Artman, J. O.; DeGraef, M.; Staley, S. W. *Phys. Rev. B* **1994**, *49*, 1135.

(11) Darvid, V. P.; Host, J. J.; Teng, M. H.; Elliott, D.; Hwang, J.; Johnson, D. L.; Mason, T. O.; Weertman, J. R. *Nature* **1995**, *374*, 620.

(12) Jonsson, T.; Svedlindh, P.; Hansen, M. F. *Phys. Rev. Lett.* **1998**, *81*, 3976.

(13) Hanson, M.; Johansson, C.; Pederson, M. S.; Morup, S. *J. Phys: Condens. Matter* **1995**, *7*, 9269.

(14) Fiorani, D.; Dorman, J. L.; Cherkaoui, R.; Tronc, E.; Lucari, F.; D'Orazio, F.; Spinu, L.; Nogues, M.; Garcia, A.; Testa, A. M. *J. Magn. Magn. Mater.* **1999**, *196*, 143.

(15) Fourgerot, F.; Chevalier, B.; Etourneau, J. *Physica B* **1997**, *230/232*, 256.

(16) Dong, X. L.; Zhang, Z. D.; Xiao, Q. F.; Zhao, X. G.; Chung, Y. C.; Jin, S. R.; Sun, W. M.; Lin, Z. J.; Zhang, Z. X.; Yang, H. *J. Mater. Sci.* **1998**, *33*, 1915.

(17) Sun, X. C.; Gutierrez, A.; Yacaman, M. J.; Dong, X. L.; Jin, S. R. *Mater. Sci. Eng. A* **2000**, *286*, 157.

(18) Sun, X. C.; Dong, X. L.; Toledo, J. A. *J. Nanosci. Nanotechnol.* **2001**, *1*, 291.

(19) Saito, Y.; Yoshikawa, T.; Okuda, M.; Fujimoto, N.; Sumiyama, K.; Suzuki, K.; Kasuya, A.; Nishina, Y. *J. Phys. Chem. Solids* **1993**, *54*, 1849.

(20) Saito, Y.; Yoshikawa, T.; Okuda, M.; Fujimoto, N.; Yamamuro, S.; Wakoh, K.; Sumiyama, K.; Suzuki, K.; Kasuya, A.; Nishina, Y. *Chem. Phys. Lett.* **1993**, *212*, 379.

(21) Bi, X. X.; Ganguly, B.; Huffman, G. P.; Huggins, F. E.; Endo, M.; Eklund, P. C. *J. Mater. Res.* **1993**, *8*, 1666.

(22) Zhang, H. *J. Phys. Chem. Solids* **1999**, *60*, 1845.

(23) Rechenberg, H. R.; Coaquira, J. A. H.; Marquina, C.; Landa, B. G.; Ibarra, M. R.; Benito, A. M.; Naser, W.; Munoz, E.; Martinez, M. T. *J. Magn. Magn. Mater.* **2001**, *226−230*, 1930.

(24) Varanda, L. C.; Jafelicci, M. J.; Goya, G. F. *J. Magn. Magn. Mater.* **2001**, *226−230*, 1933.

(25) Vijayakumar, R.; Koltypin, Y.; Felner, I.; Gedanken, A. *Mater. Sci. Eng. A* **2000**, *286*, 101.

NL0255911